Article

Osteoprotegerin is More Than a Possible Serum Marker in Liver Fibrosis: A Study into Its Function in Human and Murine Liver

Adhyatmika Adhyatmika[1,2#] (adhyatmika@ugm.ac.id), Leonie Beljaars[3#] (e.beljaars@rug.nl), Kurnia S. S. Putri[3,4] (kurnia.putri@farmasi.ui.ac.id), Habibie Habibie[6,7,8] (h.habibie@rug.nl), Carian E. Boorsma[1] (ceboorsma@gmail.com), Catharina Reker-Smit[1] (c.reker-smit@rug-nl), Burak Guney[1] (b.guney@student.rug.nl), Axel Haak[1] (a.haak@student.rug.nl), Keri A. Mangnus[1] (k.a.mangnus@student.rug.nl), Eduard Post[1] (e.post@rug.nl), Klaas Poelstra[1] (k.poelstra@rug.nl), Kim Ravnskjær[5] (ravnskjaer@bmb.sdu.dk), Peter Olinga[3] (p.olinga@rug.nl), Barbro N. Melgert[6,8*] (b.n.melgert@rug.nl)
#Equal contributions

1. Department of Pharmacokinetics, Toxicology, and Targeting, Groningen Research Institute for Pharmacy, University of Groningen, Groningen, The Netherlands
2. Faculty of Pharmacy, Gadjah Mada University, Yogyakarta, Indonesia
3. Department of Pharmaceutical Technology and Biopharmacy, Groningen Research Institute for Pharmacy, University of Groningen, Groningen, The Netherlands
4. Faculty of Pharmacy, University of Indonesia, Depok, Indonesia
5. Department of Biochemistry and Molecular Biology, University of Southern Denmark, Odense M, Denmark
6. Department of Molecular Pharmacology, Groningen Research Institute for Pharmacy, University of Groningen, Groningen, The Netherlands
7. Faculty of Pharmacy, Hasanuddin University, Makassar, Indonesia
8. Groningen Research Institute for Asthma and COPD (GRIAC), University Medical Center Groningen, Groningen, The Netherlands

*** Correspondence:**

Prof Dr Barbro N. Melgert

Department of Molecular Pharmacology

Groningen Research Institute for Pharmacy

Antonius Deusinglaan 1

9713AV Groningen

The Netherlands

Telephone number: +31 50 363 2947

E-mail address: b.n.melgert@rug.nl

Abstract: Osteoprotegerin (OPG) serum levels are associated with liver fibrogenesis and have been proposed as a biomarker for diagnosis. However, the source and role of OPG in liver fibrosis are unknown, as is the question whether OPG expression responds to treatment. Therefore, we aimed to elucidate the regulation of OPG production and its biological activity in human and mouse livers. OPG levels were significantly higher in lysates of human cirrhotic and mouse fibrotic livers compared to healthy livers. Hepatic OPG expression localized in cirrhotic collagenous bands in and around myofibroblasts. Single cell sequencing of murine liver cells showed hepatic stellate cells (HSC) to be the main producers of OPG in healthy livers. Using mouse precision-cut liver slices, we found OPG production induced by transforming growth factor β1 (TGFβ1) stimulation. Moreover, OPG itself stimulated expression of genes associated with fibrogenesis in liver slices through TGFβ1, suggesting profibrotic activity of OPG. Resolution of fibrosis in mice was associated with significantly lower OPG levels in livers as compared to their fibrotic counterparts.OPG stimulates fibrogenesis through TGFβ1 and is closely associated with the degree of fibrogenesis. It may therefore be a novel drug target for liver fibrosis or be used as a biomarker for treatment success of novel antifibrotics.

Visual abstract:

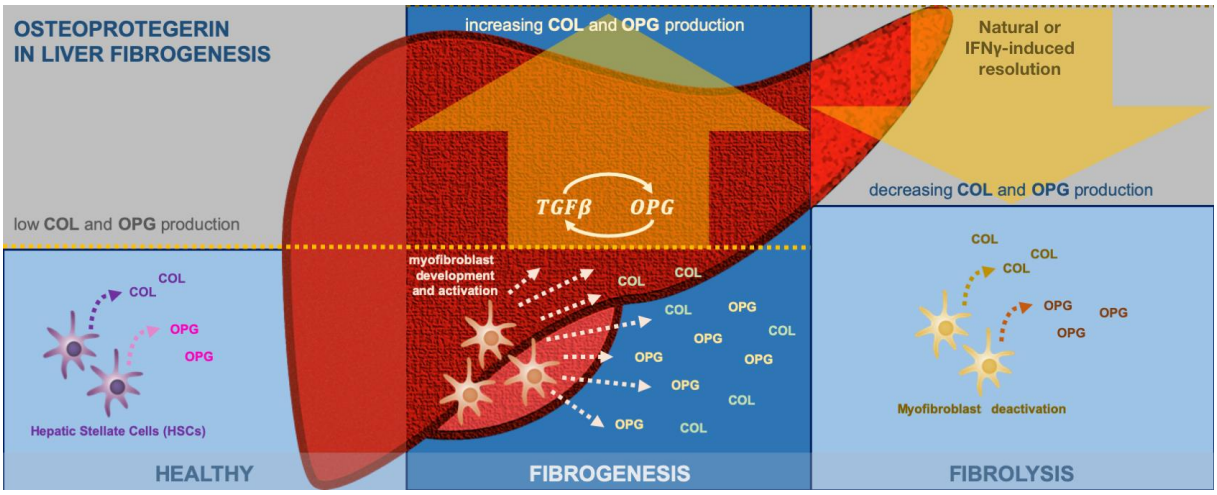

Keywords: cirrhosis; TGFβ1; CCl_4; resolution; hepatic stellate cells,; osteoprotegerin; RANKL; TRAIL

1. Introduction

Various causes of chronic damage to the liver, such as viral infections, drug toxicity, biliary problems, and high alcohol and/or fat consumption can lead to fibrosis and even cirrhosis. This process is characterized by abundant deposition of extracellular matrix in liver tissue hampering normal liver functions [1,2]. Transplantation is now the only solution when the disease has fully developed [3,4]. To date, reliable fibrosis biomarkers to diagnose disease stage in patients are scarce, especially in the early phase when pharmacological treatment is still a possible option. Another consequence of the lack of good biomarkers is the difficulty in measuring therapeutic success of antifibrotic drug candidates in patients and *in vivo* in preclinical studies [5,6].

Several studies have pointed towards osteoprotegerin (OPG) as a novel clinical biomarker associated with liver diseases [7]. Higher serum levels were measured in patients with alcoholic liver cirrhosis and primary biliary cirrhosis [8]. Furthermore, OPG was included as an additional parameter in a panel of markers in the Coopscore© to increase diagnostic accuracy of this test [9].

OPG, also known as tumor necrosis factor receptor superfamily member 11B (TNFRSF11B), is a decoy receptor for RANKL (receptor activator of nuclear factor kappa-B ligand) and TRAIL (TNF-related apoptosis-inducing ligand) [10]. OPG is known as one of the key factors of osteogenesis and is produced by osteoblasts to control osteoclast activity [11]. However, recent studies indicate that

its activities are not confined to bone homeostasis, but may be more diverse and include a role in several organ pathologies especially fibrosis [12,13] and tumor development [14,15]. Based on its scavenging activities of RANKL and TRAIL, OPG may be able to modulate fibrosis development through these ligands. However, current knowledge on the role of OPG in liver fibrosis, especially on a cellular and tissue level, is limited.

High OPG serum levels found in patients with liver fibrosis can originate from multiple organs and thus do not give any information about liver- or cell-specific regulation of OPG. We recently showed that (myo)fibroblasts are the main source of OPG production in pulmonary fibrosis[16] and Liu and colleagues showed this for cardiac fibrosis [17]. In addition, epithelial and smooth muscle cells can also produce OPG [18,19]. The cytokines TGFβ1, IL4, and IL17 were found to be stimulators of OPG production by synovial fibroblasts, whereas IFNγ could inhibit OPG production by these cells [20]. A study by Toffoli *et al.* (2011) showed *in vitro* that OPG could induce the expression of fibronectin, collagen type I, III, and IV, as well as TGFβ1 in vascular smooth muscle cells and that TGFβ1 induced the expression and triggered the release of endogenous OPG in these cells [13]. Other than this, only limited data are available about the role of OPG in fibrosis in general and particularly in liver fibrosis.

Therefore, we aimed to study: (1) liver-specific production and expression of OPG during fibrosis development *in vivo* and *in vitro*; (2) the biological role of OPG in liver tissue; (3) the response of OPG production to spontaneous resolution and drug (IFNγ)-induced resolution of fibrosis.

2. Materials and Methods

Animals. Male Balb/c mice (20-22 grams, used for the CCl_4 liver injury model) and male and female C57BL/6 mice (18-28 grams, used for precision-cut liver slices) were obtained from Harlan (Horst, The Netherlands) and were kept in cages with a 12 hours of light/dark cycle and received food and water *ad libitum*. The Institutional Animal Care and Use Committee of the University of Groningen approved the use of animals in this study (DEC5429 for CCl_4 model and DEC6416AA for precision-cut liver slices).

Human liver tissue. Anonymized residual human liver tissue samples, obtained from the Department of Hepato-Pancreato-Biliary Surgery and Liver Transplantation (University Medical Center Groningen (UMCG), the Netherlands), were collected for further analysis. In the UMCG, all patients eligible for organ transplantation are asked to sign a general consent form for the use of left-over body material (after diagnostic procedures) for research purposes. The experimental protocols were approved by the Medical Ethical Committee of the UMCG and the anonymized tissue samples were used according to Dutch guidelines. Control human liver tissue (n=5) was obtained from residual liver tissue from patients undergoing partial hepatectomy because of metastasis of colorectal carcinoma and from donor organs unsuitable for transplantation or resized donor organs. Cirrhotic human liver tissue (n=8) was obtained from patients undergoing liver transplantation. Indications for transplantation were primary sclerosing cholangitis (PSC), primary biliary cirrhosis (PBC), congenital cirrhosis, and Wilson's cirrhosis.

Liver fibrosis model. Male Balb/c mice were treated with increasing doses of CCl_4 (Fisher Scientific, Waltham, US) in olive oil intraperitoneally twice a week: first week 0.5 mL/kg, second week 0.8 mL/kg, third until eighth week 1 mL/kg. Mice were sacrificed at week 8 after developing measurable fibrosis (n=12). Control mice were sham-treated with olive oil for 8 weeks and served as healthy controls (n=11).

For the spontaneous resolution model, mice were treated with CCl_4 for 4 weeks and were then allowed to recover for 1 week and sacrificed at week 5 (n=6) as described before[22]. Control mice for this experiment were treated with CCl_4 for 4 weeks and then immediately sacrificed (n=6).

For the drug-induced resolution model, mice were treated with CCl_4 for 8 weeks and during weeks 7 and 8 mice were additionally treated with 2.5 μg/mice of IFNγ (Peprotech, Rocky Hill, US), three times a week as described before (n=6) [21]. Control mice were co-treated with saline (n=8) and both groups were sacrificed after 8 weeks of CCl_4 treatment. In all experiments serum and livers were collected for further analyses.

Precision-cut liver slices. Murine precision-cut liver slices were prepared according to standard protocols described before[23]. Slices were either not incubated (controls) or incubated in triplicate with 5 ng/mL TGFβ1 (Peprotech), 10 μM galunisertib (Selleckchem, Munich, Germany) in combination with TGFβ1, 10 ng/mL OPG (R&D Systems, Minneapolis, US), or 20 μg/mL of antibody antiRANKL, antiTRAIL, or both (antibodies-online.com) with culture medium replacements every 24 hours for a total of 48 hours (n=5-8). All collected samples were immediately snap-frozen in liquid nitrogen before storage at -80°C until further processing for analyses. Viability of the slices was assessed by measuring ATP content per milligram tissue using a bioluminescence assay kit (Sigma-Aldrich, Missouri, US) as previously reported by Hadi *et al*[24]. Slice supernatants were collected for OPG ELISA.

Cell culture. Primary human hepatic stellate cells (HHSteC, ScienCell, Carlsbad, CA, USA) were cultured in stellate cell medium containing 2% fetal bovine serum (FBS) and 1% of stellate cells growth supplement (ScienCell) in a 12-well plate initially coated with 10% human serum albumin (Sigma-Aldrich, Missouri, USA) to maintain quiescent state or uncoated to induce activation and transformation to myofibroblast-like cells and incubated with 5 ng/mL TGFβ1 (Peprotech) to simulate fibrosis. Culture supernatants were collected for OPG ELISA and cells were collected for a protein assay to correct for the number of cells in a well.

Generation of liver tissue lysates. Human or mouse liver tissue was collected in a lysis and extraction buffer containing 25 mM Tris (Sigma-Aldrich), 10 mM sodium phosphate (Sigma-Aldrich), 150 mM NaCl (Sigma-Aldrich), 0.1% SDS (Sigma-Aldrich), 1% Triton-X 100 (Sigma-Aldrich), and protease inhibitor (Thermo Scientific), snap frozen and stored at -80°C until analysis. The tissue was then mixed with the buffer using mini-bead beater for 40 seconds and centrifuged for 1 hour at 12,300 x g. Supernatants were collected and used for ELISA.

OPG analysis. OPG levels in tissue lysates, serum, and culture supernatants were measured using a murine or human OPG DuoSet® ELISA kit (Cat. No. DY459 and DY805 for mouse and human respectively, R&D Systems) according to the instructions provided by the manufacturer.

mRNA analysis. mRNA was isolated from three pooled slices per condition using a Maxwell® LEV Simply RNA Cells/Tissue kit (Promega, Madison, Wisconsin, US). Total mRNA concentration was quantified using a NanoDrop® ND-1000 Spectrophotometer (Thermo Scientific) for cDNA synthesis using a Moloney Murine Leukemia Virus Reverse Transcriptase kit (Promega) in a Mastercycler® Gradient (Eppendorf, Hamburg, Germany) with the program 10 minutes at 20°C, 30 minutes at 42°C, 12 minutes at 20°C, 5 minutes at 99°C, and 5 minutes at 20°C. Quantitative real-time PCR (qPCR) analysis was performed in triplicate with the synthesized cDNA to measure transcription of β-actin, Collagen-1α1 (Col1α1), α-smooth muscle actin (αSMA), Fibronectin (Fn1), TGFβ1, heat shock protein-47 (HSP47) and OPG using SensiMixTM SYBR® Green (Bioline, London, UK) in a 7900HT Real-Time PCR sequence detection system (Applied Biosystems, Waltham, Massachusetts, US) with primer sequences as presented in appendix A, table A1. qPCR analysis consisted of 45 cycles of 10 minutes at 95°C, 15 seconds at 95°C, and 25 seconds at 60°C (repeated for 40 times) followed by dissociation stage of 95°C for 15 seconds, 60°C for 15 seconds, and 95°C for 15 seconds. Output data were analyzed using SDS 2.4 software (Applied Biosystems) and ΔCt values were normalized to housekeeping gene β-actin and relative gene expression was calculated as $2^{-\Delta Ct}$.

Single-cell RNA sequencing and analyses. Female C57BL6/J mice were treated with vehicle or CCl_4 for 2 or 4 weeks (n=3). Sinusoid-associated CD105- and F4/80-positive cells were isolated by flow cytometry and processed for single-cell RNA-sequencing using the 10x Genomics platform. Minor cell populations and doublet cells were removed from the dataset leaving three major Louvain clusters corresponding to hepatic stellate cells, liver endothelial cells, and Kupffer cells/Monocyte-derived macrophages. Seurat (v.2.3.4) and Scanpy (v.1.4) were used for data preprocessing and Uniform Manifold Approximation and Projection (UMAP). Violin plots were generated in ggplot2 (v. 3.2.1).

Immunohistochemistry. 4 μm acetone-fixed cryosections of human or mouse liver tissue were used for histology. PBS was used to wash the sections between each step. A rabbit anti-human/mouse OPG antibody (1:200, Antibodies Online), a mouse anti-human αSMA antibody (1:500, Sigma-Aldrich), a polyclonal goat anti-collagen I (1:100, Southern Biotech), or, UK) were used, followed by secondary peroxidase-labeled goat anti-rabbit IgG or alkaline phosphatase-labeled rabbit anti-mouse IgG incubation and detection with NovaRED (Vector Laboratories, Burlingame, California, US) or BCIP/NBT (Enzo Life Science, Farmingdale, New York, US) as staining substrates. OPG and collagen I expressions were quantified using Aperio ImageScope software (Leica Biosystems), by quantifying area with positive and strong positive staining over total area of the tissue.

Statistics. All statistics were performed using GraphPad Prism 7 (La Jolla, CA, USA). Normality of data was tested using a Shapiro Wilk normality test for datasets n ≥7. If data were normally distributed, a paired or unpaired Student's t-test was used to compare two paired or unpaired groups respectively. Datasets that did not have a normal distribution were log-transformed to obtain normality and if data were still not normally distributed then nonparametric tests were used. For datasets n≤7 a Mann Whitney U or Wilcoxon test was used. When comparing multiple groups, a parametric one-way ANOVA with Holm-Sidak correction or non-parametric paired Friedman with Dunn's correction was performed depending on normality of the data. Correlations were assessed by calculating the Spearman correlation coefficient. $P<0.05$ was considered significant. Data are presented as box-and-whisker plots with individual data points for unpaired data or before-after plots for paired data.

3. Results

3.1. Osteoprotegerin expression is higher in human and murine fibrotic livers

We first quantified tissue levels of OPG in lysates of human livers and found that cirrhotic liver tissue contained significantly more OPG than control liver tissue (figure 1A). Immunohistochemical staining of human liver tissue confirmed significantly more OPG expression in sections of cirrhotic livers (figure 1B) than in sections of control livers (figure 1C). In control livers, staining for OPG expression showed a scattered pattern throughout liver parenchyma suggesting a hepatic stellate cell distribution. In cirrhotic livers, this parenchymal OPG distribution was still present in areas relatively unaffected by fibrosis, but OPG staining was predominantly present in areas of fibrosis. A double staining with αSMA, a marker of myofibroblasts, showed co-localization of OPG in αSMA-positive cells (figure 1D) and arrows in figure 1D indicate some of the double-positive cells. Note that the majority of the staining in the fibrotic areas appears to be extracellular pointing to the presence of OPG protein in excreted form or bound to extracellular matrix.

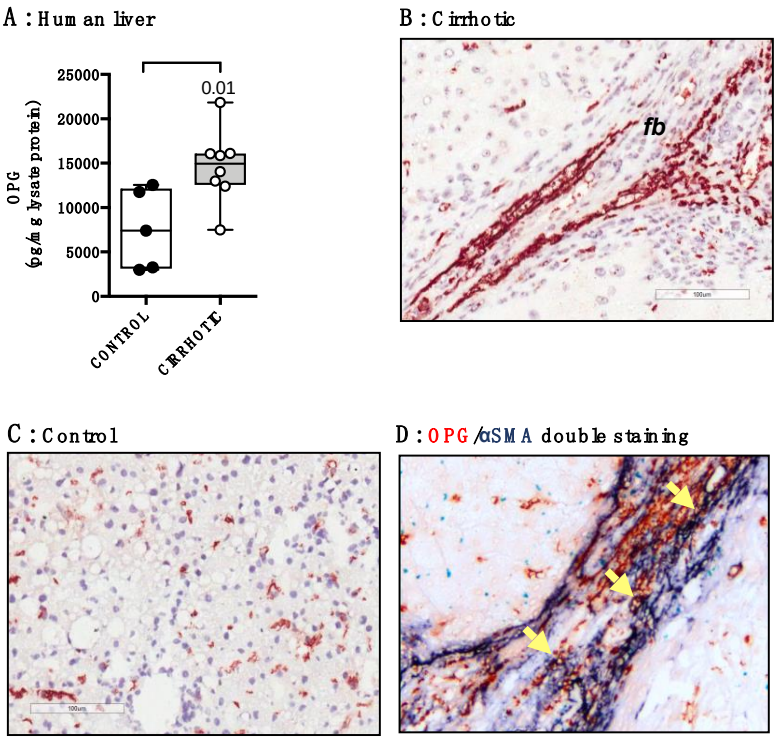

FIGURE 1. *Osteoprotegerin levels are higher in human cirrhotic livers. (A) Lysates of human cirrhotic livers (n=8) contained significantly more OPG than control livers (n=5). Groups were compared using Mann Whitney U, p<0.05 was considered significant. (B) Immunohistochemical staining showed pronounced OPG expression (bright red staining) in fibrotic bands (fb) and expression scattered throughout relatively unaffected parenchymal tissue in human cirrhotic livers (200x magnification). (C) OPG expression in control livers was only found scattered throughout the parenchyma (200x magnification). (D) The expression of OPG (red staining) in fibrotic bands in human cirrhotic livers appears to be both extracellular* and *co-localizing with αSMA-positive myofibroblasts (blue staining). Some of those double-positive cells are indicated by yellow arrows (400x magnification).*

Using a mouse model of CCl_4-induced liver fibrosis we found similar results as in human livers. We measured higher serum levels as well as liver tissue levels of OPG after 8 weeks of CCl_4-induced liver injury as compared to healthy controls (figures 2A and 2B). In control livers, staining for OPG expression was diffuse and no clear positive cells were seen as was seen for human liver tissue (figure 2C). OPG expression in murine fibrotic liver tissue predominantly localized in areas of fibrosis, similar to OPG expression in human cirrhotic livers (figure 2D). Quantification of the OPG staining confirmed the significantly higher OPG expression in fibrotic liver tissue as compared to control (figure 2E).

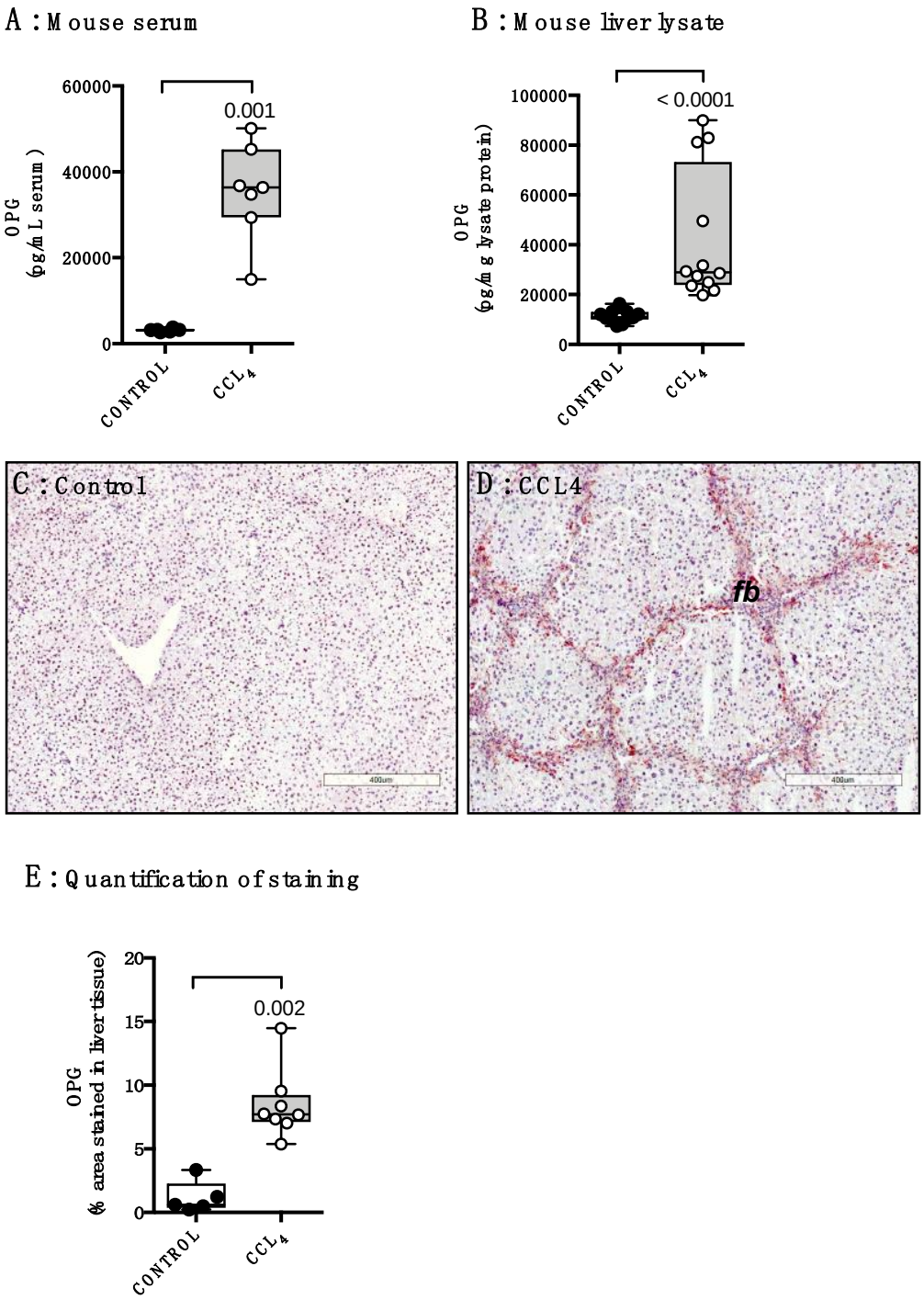

FIGURE 2. *Osteoprotegerin levels are higher in murine fibrotic livers. OPG levels were higher in serum (A) and liver tissue lysates (B) of mice treated with CCl_4 for 8 weeks compared to untreated control mice. (C) Immunohistochemical staining of OPG expression in control mouse livers showed diffuse staining and no clear positive cells (50x magnification). (D) In CCl_4-treated mouse livers pronounced OPG expression in fibrotic bands (fb) was found (50x magnification). (E) Quantification of this OPG staining showed higher expression in CCl_4-treated livers as compared to control. Groups were compared using Mann Whitney U, $p<0.05$ was considered significant.*

3.2. Hepatic stellate cells produce copious amounts of OPG

As our double staining suggested that hepatic stellate cells/myofibroblasts may be an important cellular source of liver OPG, we cultured primary human hepatic stellate cells (HHSteC) in a quiescent state in human serum albumin-coated wells and subsequently induced their activation and transformation to myofibroblast-like cells by culturing in uncoated wells and by culturing them in uncoated wells with additional TGFβ1 stimulation. Quiescent HHSteC produced copious amounts of OPG and this production was even higher when these cells transformed to myofibroblast-like cells as seen during fibrogenesis. The activation state was confirmed with increased expression of collagen 1A1 and alpha-smooth muscle actin (data not shown). However, co-incubating those activated cells with TGFβ1 did not further induce production of OPG (figure 3A).

Single cell RNA sequencing of murine liver cells showed OPG mRNA is exclusively produced by hepatic stellate cells (HSCs) and not by liver endothelial cells (LECs), Kupffer cells (KCs) or monocytes-derived macrophages (MDMs, figure 3B). Treatment of mice with CCl_4 for 2 weeks or 4 weeks resulted in a decline of OPG mRNA expression in hepatic stellate cells as compared to healthy control mice (figure 3C).

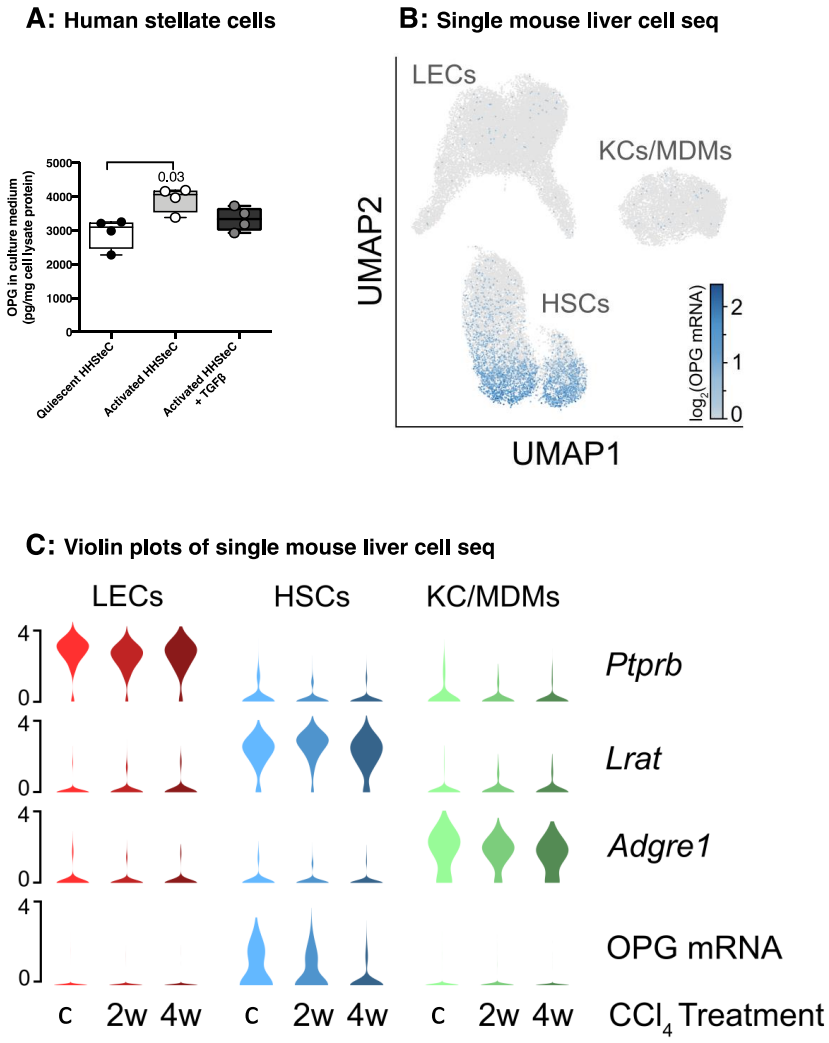

FIGURE 3. *Human and murine hepatic stellate cells produce OPG. (A) Activated human hepatic stellate cells (HHSteC) produced significantly more OPG than quiescent HHSteC, but not when they were also treated with TGFβ1. HHSteC were activated by culturing on uncoated plastic. Groups were compared using*

a Friedman test with a Dunn's correction for multiple testing and $p<0.05$ was considered significant. (B) UMAP showing murine hepatic stellate cells (HSCs), liver endothelial cells (LECs), and Kupffer cells (KCs)/Monocyte-derived macrophages (MDMs) overlaid with log_2 OPG mRNA expression. The minor HSC population to the right correspond to quiescent HSCs mainly derived from vehicle-treated control mice. (C) Log_2 expression of OPG and cell type markers lecithin retinol-acyltransferase (Lrat), protein tyrosine phosphatase receptor type B (Ptprb) and glycoprotein F4/80 (Adgre1). OPG mRNA expression in HSCs was less after treatment with CCl_4 for 2 weeks (2w) or 4 weeks (4w) compared to vehicle-treated mice (c).

3.3. TGFβ1 induces OPG mRNA and protein production in murine precision-cut liver slices, which correlates with other markers of fibrosis

To verify liver-specific production of OPG and to investigate its production during fibrogenesis in more detail, we stimulated mouse precision-cut liver slices with TGFβ1 to induce a fibrotic process. We found that liver tissue can express and produce OPG itself and additionally that TGFβ1 stimulation of liver slices resulted in significantly higher OPG mRNA expression, which correlated (Spearman $\varrho=0.63$, $p=0.02$) with higher OPG protein excretion as compared to untreated control slices (figures 4A-C). This higher production of OPG after TGFβ1 stimulation was accompanied by significantly more expression of the fibrosis-associated genes Col1α1, αSMA, Fn1, and TGFβ1 itself as compared to untreated control slices, but not HSP47 (figure 4D-H). Moreover, OPG mRNA expression significantly correlated with mRNA expressions of Col1α1 and HSP47 (figure 4I-J) and OPG protein expression significantly correlated with Fn1 and TGFβ1 mRNA expressions (figure 4K-L). All treatments did not compromise viability of tissue slices as no significant decrease of ATP content was found in all treatment groups as compared to untreated controls after 48 hours of incubation (Figure A1 of appendix A).

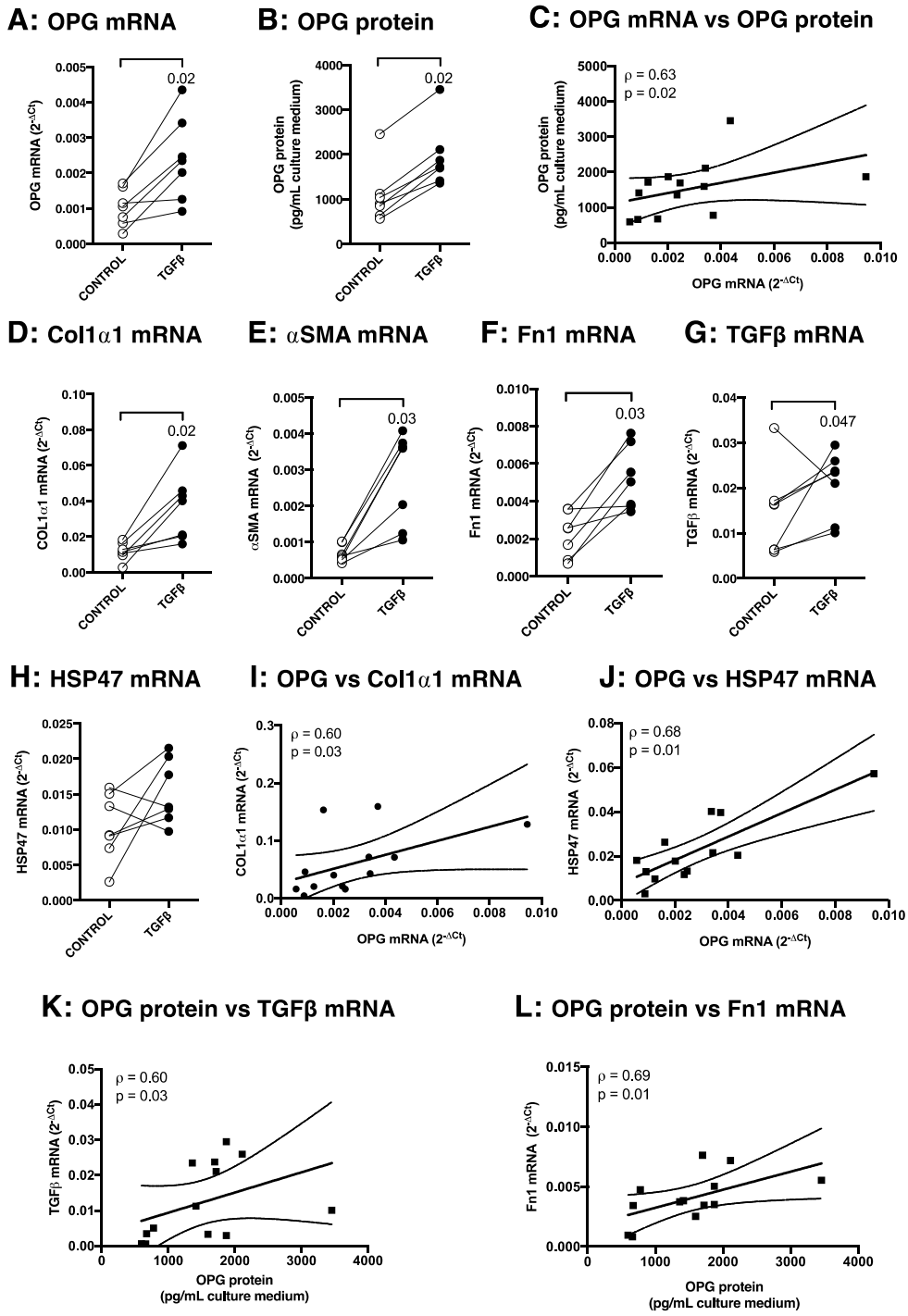

FIGURE 4. *TGFβ1 induces OPG expression as well as various fibrosis-associated markers in murine liver slices. When murine liver slices were treated with 5 ng/ml TGFβ1, significantly more OPG mRNA (A) and OPG protein excretion (B) were observed, which correlated closely with each other (C, Spearman ρ=0.63, p=0.02). This higher OPG production was accompanied by higher mRNA expression levels of fibrosis-associated markers Col1α1 (D), αSMA (E), Fn1 (F), and TGFβ1 (G), but not HSP47 (H). OPG mRNA expression correlated closely with Col1α1 (I) and HSP47 (J) mRNA expression, while OPG protein secretion correlated with TGFβ1 (K) and Fn1 (L) mRNA expression. Groups were compared using Wilcoxon, correlations were calculated using a Spearman correlation test, and p<0.05 was considered significant. For the correlations, data from control and TGFβ1-stimulated slices of figure 5 were also added.*

3.4. OPG treatment of mouse precision-cut liver slices results in higher expression of fibrosis-associated markers through TGFβ1

To investigate the biological role of OPG in liver fibrosis, murine liver slices were treated with OPG itself and compared to the effects of incubation with positive control TGFβ1. Stimulation with 10 ng/mL OPG resulted in significantly higher mRNA expressions of Col1α1, HSP47, Fn1, αSMA, and most notably TGFβ1 as compared to controls, (figures 5A-E). These effects were similar to stimulation with TGFβ1, which was included as a positive control, although TGFβ1 also significantly induced expression OPG mRNA, while this was a trend for treatment with OPG itself (figure 5F).

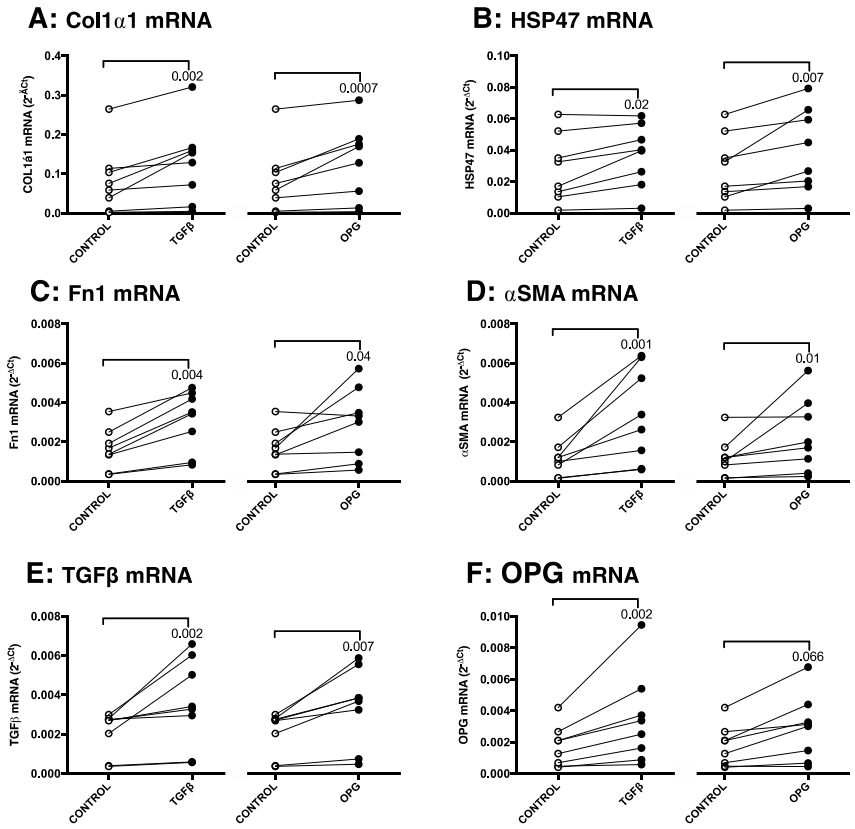

FIGURE 5. *OPG treatment of liver slices results in higher expression of fibrosis-associated markers. Treatment of mouse precision-cut liver slices with 10 ng/ml OPG resulted in higher mRNA expressions of fibrosis-associated markers Col1α1 (A), HSP47 (B), Fn1 (C), αSMA (D), and TGFβ1(E) just like treatment with positive control TGFβ1. OPG itself was only significantly upregulated by TGFβ1 treatment and not significantly after OPG treatment (F). Groups were compared using a Friedman test with a Dunn's correction for multiple testing and p<0.05 was considered significant.*

We then investigated whether this profibrotic activity of OPG could be explained by its upregulation of TGFβ1 expression. We therefore inhibited TGFβ1 signalling by using galunisertib (LY2157299), a TGFβ1 receptor kinase inhibitor. We found that inhibiting TGFβ1-signalling by galunisertib in slices treated with TGFβ1 resulted in significantly lower expression of Col1α1, Fn1, and αSMA mRNA and a trend towards lower HSP47 mRNA expression (p=0.07) compared to liver slices treated with only TGFβ1 alone (figure 6A-E). A similar pattern was seen for slices treated with galunisertib and OPG as compared to slices only treated with OPG, with Col1α1, HSP47, αSMA being significantly inhibited, and no significant effects on Fn1 (figure 6A-D). Galunisertib did not affect the expression of TGFβ1 mRNA expression after TGFβ1 or OPG treatment (figure 6E)

and treatment with galunisertib on its own did not affect expression of all genes as compared to nontreated controls.

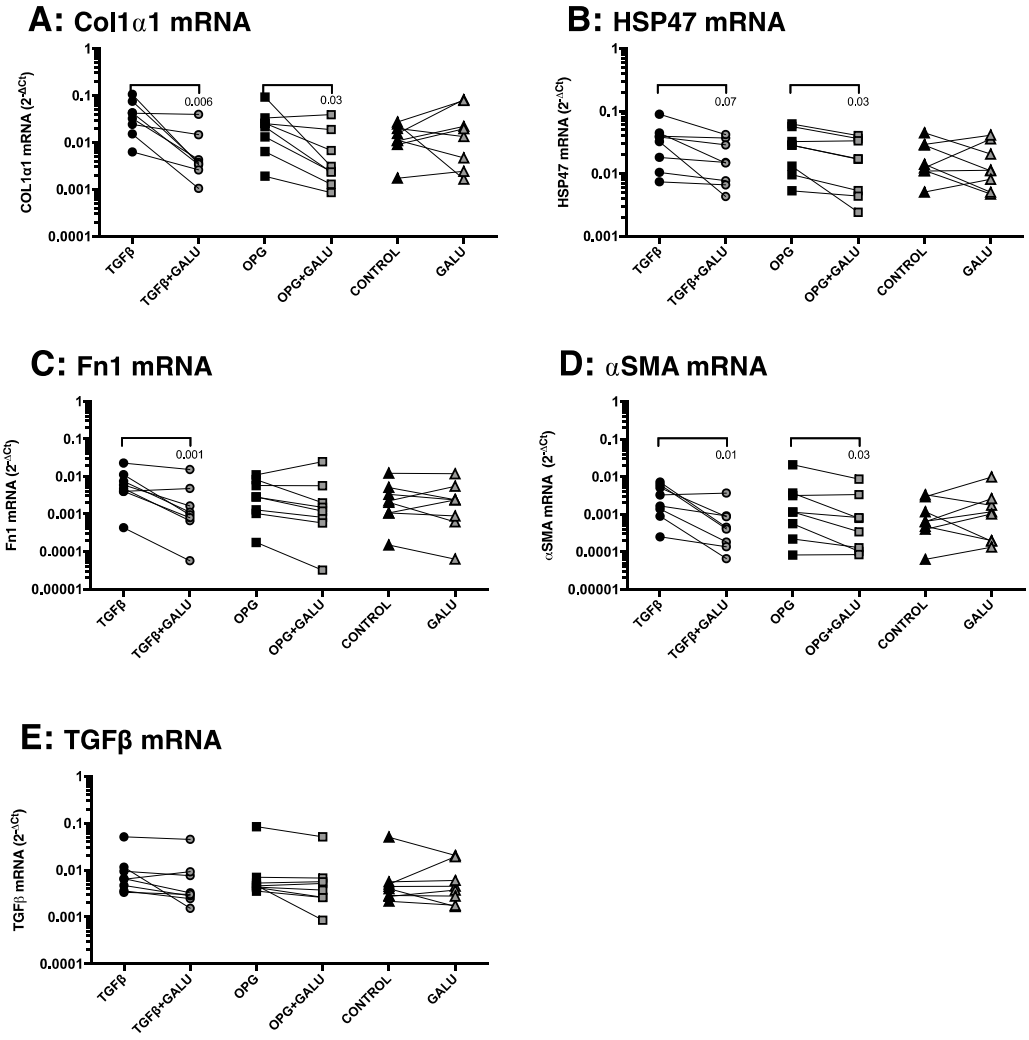

FIGURE 6. *Inhibition of TGFβ1-signaling results in lower expression of fibrotic markers in slices treated with TGFβ1 or OPG. Inhibition of TGFβ signaling by treating with galunisertib (Galu) abrogated the profibrotic effects of both TGFβ1 (positive control) and OPG. Groups with parametric data were compared using a one-way ANOVA with a Holm-Sidak's correction for multiple testing and groups with nonparametric data with a Friedman test with a Dunn's correction for multiple testing and $p<0.05$ was considered significant.*

To study whether the profibrotic activity of OPG is related to its inhibition of RANKL and TRAIL activities, slices were incubated with neutralizing antibodies against RANKL and TRAIL to mimic both known OPG scavenging activities. Again, mRNA expressions of Col1α1, HSP47, Fn1, αSMA, and TGFβ1 were used as outcome parameters. We found that incubation with the combination anti-RANKL and anti-TRAIL neutralizing antibodies more or less mimicked the results found for treatment with OPG. OPG treatment resulted in significantly more Col1α1, Fn1, and αSMA, with trends towards more HSP47 and TGFβ1 mRNA, while anti-RANKL/TRAIL treatment resulted in significantly more Col1α1, HSP47, and αSMA, with trends towards more Fn1 and TGFβ1 mRNA (figure 7A-E).

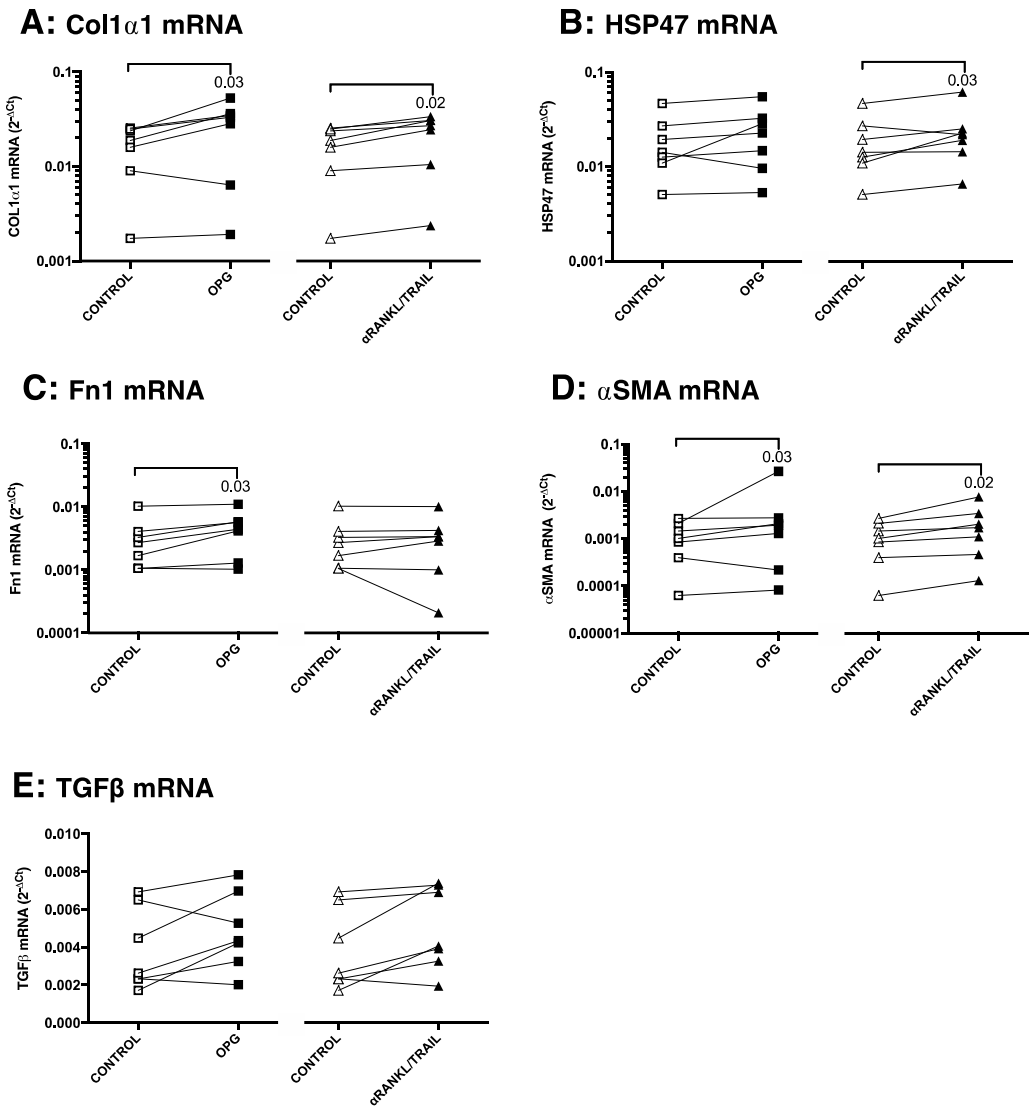

FIGURE 7. *Treatment with neutralizing antibodies against RANKL and TRAIL resembles the effects of OPG. Groups were compared using a Friedman test with a Dunn's correction for multiple testing and $p<0.05$ was considered significant.*

3.5. OPG expression responds to spontaneous and drug-induced fibrosis resolution

To study the response of OPG production to resolution of fibrosis we used two mouse models of fibrosis resolution (spontaneous and drug-induced). In mice with CCl_4-induced liver fibrosis, we induced spontaneous resolution by cessation of CCl_4 for one week after four weeks of CCl_4 treatments and we induced resolution by treatment with the antifibrotic cytokine IFNγ in the last two weeks of eight weeks of CCl_4 treatments. Both methods of resolution induction resulted in significantly lower collagen type I deposition in liver tissue as was published by us before [21,22]. Importantly, the lower amount of collagen deposition, shown in these previous studies, was accompanied by a concomitant significantly lower OPG expression in liver tissue (figures 8A-B).

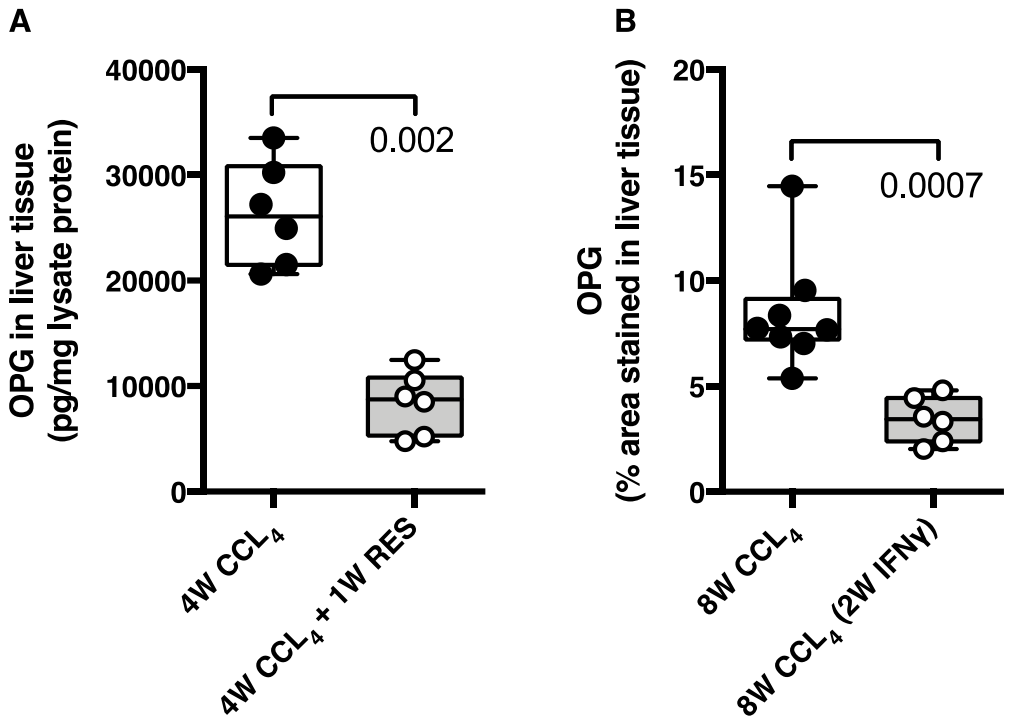

FIGURE 8. *OPG responds to spontaneous and drug (IFNγ)-induced resolution. In vivo spontaneous (A) and IFNγ-induced (B) resolution of CCl_4-induced liver fibrosis in mice resulted in lower OPG levels in liver tissue as compared to their respective controls, which was accompanied by lower collagen type I deposition as was published by us before [21,22]. Groups were compared using Mann-Whitney U, $p<0.05$ was considered significant.*

4. Discussion

OPG has previously been associated with liver fibrosis and has been included in a panel of serum markers to assess liver fibrosis severity [8,9]. We now show that it is produced in healthy liver tissue by hepatic stellate cells and that its expression in liver tissue is stimulated by exposure to TGFβ1. Moreover, OPG itself appears profibrotic through neutralizing RANKL and/or TRAIL and upregulation of TGFβ1 expression and may therefore be a novel target for pharmacological treatment. In addition, we have shown that OPG production decreases when fibrosis resolves, suggesting it may also be used as (serum) biomarker to assess treatment success.

We first assessed whether the previously reported elevated levels of OPG in liver fibrosis were a result of elevated production within the fibrotic liver or coming from other parts of the body [8,9]. We indeed found higher levels of OPG in both human and murine liver tissue lysates of cirrhotic/fibrotic livers as compared to healthy tissues. To confirm OPG was genuinely produced in liver tissue we subsequently used liver slices and we found that after stimulation with TGFβ1, OPG production increased parallel to the induction of early fibrosis in these slices. This proved that liver tissue itself is capable of producing OPG under the influence of a fibrotic stimulus. In addition, immunohistochemical staining and *in vitro* HHSteC studies indicate that myofibroblasts and activated HHSteC are an important source of OPG within the liver.

Interestingly, our single liver cell sequencing data confirmed clear production of OPG by hepatic stellate cells in healthy mouse livers, but a loss of OPG production by hepatic stellate cells in fibrotic livers. There are several possible explanations for this puzzling finding. Firstly, hepatic stellate cells could lose the ability to produce OPG but other mesenchymal cells develop/move into the liver that produce the copious amounts of OPG we found in fibrotic liver tissue. The cells isolated for single cell sequencing were enriched for endothelial cells, macrophages, monocytes and hepatic stellate

cells and we may therefore have missed the cells that start producing excess amounts of OPG, i.e. myofibroblasts of other origins such as fibrocytes or fibroblasts. Another explanation is that the activated hepatic stellate cells that produce OPG are more difficult to isolate from fibrotic tissue and are therefore lost for sequencing. Our immunohistochemistry results show that the main producers of OPG in fibrotic liver tissue are in the fibrotic bands and may therefore be harder to isolate without damage and may thus have not been adequately included in our analysis.

Importantly, using the data generated by single liver cell sequencing, and our immunohistochemistry stainings we found no evidence for OPG production by Kupffer cells or endothelial cells. This is in contrast with work from Sakai et al (2012) who showed low-level production by Kupffer cells after TNFα stimulation[26]. Our single cell sequencing data did not pick up any OPG expression in Kupffer cells, but we did not specifically stimulate with TNFα, which may explain the differences found.

An important question that arises is why hepatic OPG increases during fibrogenesis of the liver. Therefore, we first assessed whether OPG itself exerts biological activities on liver tissue. We found higher mRNA expressions of all fibrosis markers tested after treatment of liver slices with OPG, although the extent of the profibrotic effect of OPG was more variable than TGFβ1. This suggests that OPG has profibrotic activities in the liver and may therefore be involved in generating a profibrotic environment. The next question we addressed was how OPG could exert such a profibrotic effect. Our studies with galunisertib indicate that the upregulation of TGFβ1 expression by OPG is most probably responsible for this effect as galunisertib, a TGFβ1 receptor kinase inhibitor, completely abolished the profibrotic effect of OPG. That left us with the question how OPG can upregulate TGFβ1 expression. To date no receptor or signaling properties of OPG itself have been reported[27]. Therefore, we hypothesized that its TGFβ1-stimulating properties are the result of either scavenging RANKL and/or TRAIL as these ligands have been reported to bind to OPG [28]. Our results using neutralizing antibodies against RANKL and TRAIL show that these have more or less the same effects as OPG, suggesting that either or both play a role in preventing fibrosis. Interestingly, RANKL was reported to play a role in hepatic cellular repair mechanisms. Sakai et al (2012) showed high expression of the receptor for RANKL, i.e. RANK, on hepatocytes and subsequently showed that RANKL treatment can induce cell proliferation and thus reduce liver injury in a model of ischemia/reperfusion damage [26]. Preliminary studies by us treating liver slices with RANKL seem to indicate RANKL can indeed induce proliferation of cholangiocytes/hepatocyte progenitors, which will have to be further investigated.

TRAIL is a known inducer of apoptosis through its death receptors DR4 and DR5 [30]. Expression of TRAIL was shown on activated stellate cells in cirrhotic livers but not on quiescent ones [31]. Therefore, TRAIL expression may be a mechanism to induce apoptosis of myofibroblasts after tissue repair is finished and the continued presence of myofibroblasts in no longer needed. Our studies have clearly shown that activated HHSteC and (myo)fibroblasts produce OPG and therefore may be able to prevent apoptosis and maintain fibrotic conditions through this production of OPG [32].

As OPG production appears to be closely linked to the process of liver fibrogenesis, we hypothesized that OPG may also serve as a marker to assess resolution of the disease. To verify this, we studied OPG expression in two resolution models: one model of spontaneous resolution, and one model with IFNγ as an antifibrotic drug [21]. The induction of liver fibrosis in mice *in vivo* using CCl_4 has been shown to be reversible when administration of CCl_4 is stopped. We previously found that after 4 weeks of CCl_4 administration and one-week cessation of CCl_4 administration the deposition of collagen in liver tissue was markedly lower than animals that had received CCl_4 for 4 weeks (published in [22]). Interestingly, we now show that at the same time OPG expression was also lower after one week of regeneration, suggesting OPG expression decreases when the liver is regenerating. A similar pattern was also found in an experiment of eight weeks of CCl_4

administration, in which the animals were treated with IFNγ in the last two weeks of the fibrosis-inducing period. We have previously shown that treatment with IFNγ resulted in a significant reduction of fibrosis in liver tissue indicating resolution of disease [21]. We now show that this resolution is accompanied by less OPG expression in liver tissue. These *in vivo* results suggest that OPG expression is not only linked to fibrosis development, but that it can also be used to detect resolution of disease. This makes it a tempting candidate for biomarker studies as development of novel drugs against liver fibrosis is severely hampered by the lack of biomarkers to detect efficacy of treatments [33].

5. Conclusions

Our data show that liver fibrosis is accompanied by higher production of OPG in liver tissue, particularly in response to TGFβ1. Hepatic stellate cells appear to be the main source of OPG, which has profibrotic abilities through neutralization of RANKL and/or TRAIL and upregulation of TGFβ1 expression. Spontaneous or drug-induced resolution of fibrosis is accompanied by lower expression of OPG. We therefore conclude that OPG may be a novel drug target and/or biomarker for liver fibrosis.

Author Contributions: Conceptualization, Leonie Beljaars and Barbro Melgert; Data curation, Adhyatmika Adhyatmika, Leonie Beljaars, Kurnia Putri, Habibie Habibie, Carian Boorsma, Burak Guney, Axel Haak, Keri Mangnus, Kim Ravnskjær and Barbro Melgert; Formal analysis, Adhyatmika Adhyatmika, Kurnia Putri, Carian Boorsma, Kim Ravnskjær and Barbro Melgert; Funding acquisition, Peter Olinga and Barbro Melgert; Investigation, Adhyatmika Adhyatmika, Leonie Beljaars, Habibie Habibie, Carian Boorsma and Barbro Melgert; Methodology, Adhyatmika Adhyatmika, Leonie Beljaars, Kurnia Putri, Habibie Habibie, Carian Boorsma, Catharina Reker-Smit, Eduard Post, Kim Ravnskjær and Barbro Melgert; Project administration, Barbro Melgert; Resources, Barbro Melgert; Software, Barbro Melgert; Supervision, Leonie Beljaars, Klaas Poelstra, Peter Olinga and Barbro Melgert; Validation, Leonie Beljaars and Barbro Melgert; Visualization, Leonie Beljaars, Kim Ravnskjær and Barbro Melgert; Writing – original draft, Adhyatmika Adhyatmika and Barbro Melgert; Writing – review & editing, Leonie Beljaars, Kurnia Putri, Habibie Habibie, Carian Boorsma, Catharina Reker-Smit, Burak Guney, Axel Haak, Keri Mangnus, Eduard Post, Klaas Poelstra, Kim Ravnskjær, Peter Olinga and Barbro Melgert.

Funding: AA and HH were supported by a LPDP fellowship from the Indonesian government.

Conflicts of Interest: The authors declare no conflict of interest. The funders had no role in the design of the study; in the collection, analyses, or interpretation of data; in the writing of the manuscript, or in the decision to publish the results.

Appendix A

TABLE A1. Sequences of the primers used in this study

β-actin	ATCGTGCGTGACATCAAAGA	ATGCCACAGGATTCCATACC
Col1α1	TGACTGGAAGAGCGGAGAGT	ATCCATCGGTCATGCTCTCT
αSMA	ACTACTGCCGAGCGTGAGAT	CCAATGAAAGATGGCTGGAA
Fn1	CGGAGAGAGTGCCCCTACTA	CGATATTGGTGAATCGCAGA
OPG	ACAGTTTGCCTGGGACCAAA	CTGTGGTGAGGTTCGAGTGG
TGFβ1	AGGGCTACCATGCCAACTTC	GTTGGACAACTGCTCCACCT
HSP47	AGGTCACCAAGGATGTGGAG	CAGCTTCTCCTTCTCGTCGT

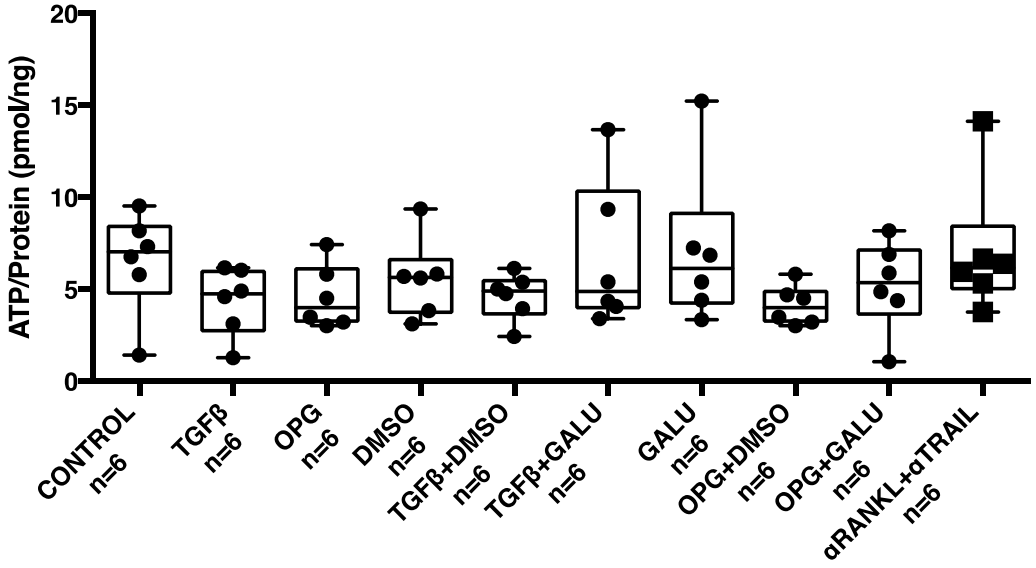

FIGURE A1. Treatments did not compromise viability of mouse liver slices. The treatments used in these studies did not significantly compromise the viability of the mouse liver slices (n=6, Kruskal-Wallis test corrected for multiple testing).

References

1. Friedman, S.L. Liver fibrosis – from bench to bedside. *Journal of Hepatology* **2003**, *38*, S38-S53.
2. Bataller, R.; Brenner, D.A. Liver fibrosis. *Journal of Clinical Investigation* ***2005***; *115(2)*, 209-218.
3. Ge, P. S.; Runyon, B.A. Treatment of patients with cirrhosis. *New England Journal of Medicine* **2016**, *375*, 767-777.
4. Schuppan, D.; Kim, Y.O. Evolving therapies for liver fibrosis. *Journal of Clinical Investigation* **2013**, *123(5)*, 1887-1901.
5. Fallatah, H.I. Noninvasive biomarkers of liver fibrosis: An overview. *Advances in Hepatology* **2014**, *article ID 357287*.
6. Motola, D.L.; Caravan, P.; Chung, R.T.; Fuchs, B.C. Noninvasive biomarkers of liver fibrosis: Clinical applications and future directions. *Current Pathobiology Reports* **2015**, *2(4)*, 245-256.
7. Yilmaz, Y.; Yonal, O.; Kurt, R.; Oral, A.Y.; Eren, F.; Ozdogan, O.; Ari, F.; Celikel, C.A.; Korkmaz, S.; Ulukaya, E.; Imeryuz, N.; Kalayci, C.; Avsar, E. Serum levels of osteoprotegerin in the spectrum of nonalcoholic fatty liver disease. *Scandinavian Journal of Clinical and Laboratory Investigation* **2010**, *70*, 541-546.
8. García-Valdecasas-Campelo, E.; González-Reimers, E.; Santolaria-Fernández, F.; De La Vega-Prieto, M.J.; Milena-Abril, A.; Sanchez-Perez, M.J.; Martínez-Riera, A.; Gómez-Rodríguez, M.D.L.A. Serum osteoprotegerin and RANKL levels in chronic alcoholic liver disease. *Alcohol and Alcoholism* **2006**, *41(3)*, 261-266.
9. Bosselut, N.; Taibi, L.; Guéchot, J.; Zarski, J.P., Sturm, N.; Gelineau, M.C.; Poggi, B.; Thoret, S.; Lasnier, E.; Baudin, B.; Housset, C.; Vaubourdolle, M.; The ANRS HCEP 23 Fibrostar Group. Including osteoprotegerin and collagen IV in a score-based blood test for liver fibrosis increases diagnostic accuracy. *Clinica Chimica Acta* **2013**, *415*, 63-68.
10. Vitovski, S.; Phillips, J.S.; Sayers, J.; Croucher, P.I. Investigating the interaction between osteoprotegerin and receptor activator of NFκB or tumor necrosis factor-related apoptosis-inducing ligand: evidence for a pivotal role for osteoprotegerin in regulating two distinct pathways. *Journal of Biological Chemistry* **2007**, *282(43)*, 31601-31609.
11. Boyce, B.F.; Xing, L. Biology of RANK, RANKL, and osteoprotegerin. *Arthritis Research Therapy* **2007**, *9(Suppl 1)*, S1.
12. Bock, O.; Loch, G.; Schade, U.; Büsche, G.; von Wasielewski, R.; Wiese, B.; Kreipe, H.; Osteosclerosis in advanced chronic idiopathic myelofibrosis is associated with endothelial overexpression of osteoprotegerin. *British Journal of Haematology* **2005**, *130*, 76-82.
13. Toffoli, B.; Pickering, R.J.; Tsorotes, D.; Wang, B.; Bernardi, S.; Kantharidis, P.; Fabris, B.; Zauli, G.; Secchiero, P.; Thomas, M.C. Osteoprotegerin promotes vascular fibrosis via a TGF-β1 autocrine loop. *Atherosclerosis* **2011**, *218*, 61-68.
14. Cross, S.S.; Yang, Z.; Brown, N.J.; Balasubramanian, S.P.; Evans, C.A.; Woodward, J.K.; Neville-Webbe, H.L.; Lippitt, J.M.; Reed, M.W.R.; Coleman, R.E.; Holen, I. Osteoprotegerin (OPG)—a potential new role in the regulation of endothelial cell phenotype and tumour angiogenesis? *International Journal of Cancer* **2006**, *118*, 1901-1908.
15. Holen, I.; Cross, S.S.; Neville-Webbe, H.L.; Cross, N.A.; Balasubramanian, S.P.; Croucher, P.I.; Evans, C.A.; Lippitt, J.M.; Coleman, R.E.; Eaton, C.L. Osteoprotegerin (OPG) expression by breast cancer cells in vitro and breast tumours in vivo – a role in tumour survival? *Breast Cancer Research Treatment* **2005**, *92*, 207-215.
16. Boorsma, C.E.; Draijer, C.; Cool, R.; Brandsma, C.; Nossent, G.; Brass, D.M.; Timens, W.; Melgert, B.M. A possible role for the RANK/RANKL/OPG axis in pulmonary fibrosis. *American Journal of Respiratory Critical Care Medicine* **2014**, *189*, A1252.
17. Liu, W.; Feng, W.; Wang, F.; Li, W.; Gao, C.; Zhou, B.; Ma, M.; Osteoprotegerin/RANK/RANKL axis in cardiac remodelling due to immuno-inflammatory myocardiac disease. *Experimental and Molecular Pathology* **2008**, **84(3)**, 213-217.
18. Vidal, K.; Serrant, P.; Schlosser, B.; van den Broek, P.; Lorget, F.; Donnet-Hughes, A. Osteoprotegerin production by human interstitial epithelial cells: A potential regulator of mucosal immune responses. *American Journal of Physiology—Gastrointestinal and Liver Physiology* **2004**, *287(4)*, G836-844.
19. Zhang, J.; Fu, M.; Myles, D.; Zhu, X.; Du, J.; Cao, X.; Chen, Y.E. PDGF induces osteoprotegerin expression in vascular smooth muscle cells by multiple signal pathways. *FEBS Letters* **2002**, 521, 180-184.

20. Tunyogi-Csapo, M.; Kis-Toth, K.; Radacs, M.; Farkas, B.; Jacobs, J.J.; Finnegan, A.; Mikecz, K.; Glant, T.T. Cytokine-controlled RANKL and osteoprotegerin expression by human and mouse synovial fibroblasts (Fibroblast-mediated pathologic bone resorption). *Arthritis and Rheumatism* **2008**, *58(8)*, 2397-2408.
21. Bansal, R.; Prakash, J.; Post, E.; Beljaars, L.; Schuppan, D.; Poelstra, K. Novel engineered targeted interferron-gamma blocks hepatic fibrogenesis in mice. *Hepatology* **2011**, *54(2)*, 586-596.
22. Beljaars, L.; Schippers, M.; Reker-smit, C.; Martinez, F.O.; Helming, L.; Poelstra, K.; Melgert, B.N. Hepatic localization of macrophage phenotypes during fibrogenesis and resolution of fibrosis in mice and humans. *Frontiers in Immunology* **2014**, *5*, Article 430, 1-11.
23. De Graaf, I.A.M.; Olinga, P.; De Jager, M.H.; Merema, M.T.; De Kanter, R.; Van de Kerkhof, E.G.; Groothuis, G.M.M. Preparation and incubation of precision-cut liver and intestinal slices for application in drug metabolism and toxicity studies. *NATURE Protocols* **2010**, *5*, 1540-1551
24. Hadi, M.; Chen, Y.; Starokozhko, V.; Merema, M.T.; Groothuis, G.M.M. Mouse precision-cut liver slices as an ex vivo model to study idiosyncratic drug-induced liver injury. *Chemical Research in Toxicology* **2012**, *25(9)*, 1938-1947.
25. Beckstead, J.H. A simple technique for preservation of fixation-sensitive antigens in paraffin-embedded tissues. *Journal of Histochemistry and Cytochemistry* **1994**, *42(8)*, 1127-1134
26. Sakai, N.; Van Sweringen, H.L.; Schuster, R.; Blanchard, J.; Burns, J.M.; Tevar, A.D.; Edwards, M.J.; Lentsch, A.B. Receptor Activator of Nuclear Factor-κB ligand (RANKL) protects against hepatic ischemia/reperfusion injury in mice. *Hepatology* **2012**, *55(3)*, 888-897.
27. Dawson, S.; Lawrie, A. From bones to blood pressure, developing novel biologic approaches targeting the osteoprotegerin pathway for pulmonary vascular disease. *Pharmacology and Therapeutics* **2017**, *169*, 78-82.
28. Beljaars, L.; Boorsma, C.E.; Guney, B.; Poelstra, K.; Melgert, B.N. A new communication system regulating extracellular matrix in liver fibrosis: RANK/RANKL/OPG [Abstract]. *Hepatology* **2014**, *60(Suppl 1)*, 584A-584A.
29. Michalopoulos, G.; Khan, Z. Liver stem cells: Experimental findings and implications for human liver disease. *Gastroenterology* **2015**, *149(4)*, 876-82
30. Lemke, J.; von Karstedt, S.; Zinngrebe, J.; Walczak, H. Getting TRAIL back on track for cancer therapy. *Cell Death and Differentiation* **2014**, *21*, 1350-1364.
31. Taimr, P.; Higuchi, H.; Kocova, E.; Rippe, R.A.; Friedman, S.; Gores, G.J. Activated stellate cells express the TRAIL receptor-2/death receptor-5 cancer-specific apoptosis within a therapeutic window. *Hepatology* **2007**, *45*, 649-658.
32. Chamoux, E.; Houde, N.; L'Eriger, K.; Roux, S. Osteoprotegerin decreases human osteoclast apoptosis by inhibiting the TRAIL pathway. *Journal of Cellular Physiology* **2008**, *216(2)*, 536-542.
33. Marshall, R.P.; Simpson, J.K.; Lukey, P.T. Strategies for biomarker discovery in fibrotic disease. *Biochimica et Biophysica Acta – Molecular Basis of Disease* **2013**: 1079-1087.